Kinetics and Catalysis, Vol. 43, No. 1, 2002, pp. 99–106. Translated from Kinetika i Kataliz, Vol. 43, No. 1, 2002, pp. 108–115.

Peculiarities of Catalytic Oxidation of Ethane by Nitrous Oxide on ZSM-5 Type Zeolites Containing Iron Ions in Different Localization Sites

A. V. Kucherov, V. D. Nissenbaum, T. N. Kucherova, and L. M. Kustov

Zelinskii Institute of Organic Chemistry, Russian Academy of Sciences, Moscow, 119991 Russia

Received February 23, 2001

Abstract—The temperature dependence of the Fe-HZSM-5 activity and selectivity in the process of catalytic oxidation of ethane by the excess of N_2O at 250–350°C exhibits a pronounced hysteresis. The oxidized catalysts free from condensation products are active only in the complete oxidation of ethane. At low temperatures of the reaction of the $C_2H_6 + N_2O$ mixture with the catalyst, coke formation takes place and the coordination state of iron ions differs from the initial sample. Under these conditions, the process of complete oxidation of ethane is essentially suppressed and the process of oxidative dehydrogenation dominates. The catalytic properties of iron-containing zeolites prepared either by direct synthesis or by introduction of iron ions into the cationic positions of H[Al]ZSM-5 are quite similar, because irreversible formation of new iron species considerably different from the initial species takes place during the catalytic reaction on both series of samples. The activity of HZSM-5 containing trace amounts of iron is much lower than that of iron-containing samples.

INTRODUCTION

Heterogeneous catalytic oxidation of lower alkanes continues to attract significant interest in connection with two important industrial problems. One is related to complete oxidation for the removal of traces of hydrocarbons in the processes of production of extra pure gases. The main progress in this field is connected with the use of highly dispersed oxide- and zeolite-based catalysts. The second, more important, problem is connected with the production of oxygenates, ethylene, and aromatic compounds by the partial oxidation of a cheap and available feedstock, in particular methane and ethane. However, in spite of numerous research efforts, no process suitable for industrial application has been developed so far [1].

Experiments with different oxidizing agents (O_2, O_3, NO, and N_2O) have shown that the use of nitrous oxide instead of oxygen in the process of oxidation of ethane enables one to increase the selectivity to the partial oxidation products [2–6]. Adsorption of N_2O on iron-containing ZSM-5 zeolites leads to the formation of active oxygen species capable of participating in benzene oxidation into phenol at low temperatures with a high selectivity [7–10]. Therefore, the purpose of this work was to elucidate the mechanisms of N_2O decomposition and ethane oxidation by N_2O on ZSM-5 zeolites containing iron ions in different localization sites and to compare the results with those obtained earlier for the Cu-HZSM-5 system [11].

EXPERIMENTAL

Catalysts

Fe-H[Al]ZSM-5. Catalysts containing 0.5 and 2.1 wt % of iron were prepared by introducing Fe^{3+} ions into the cationic positions of H[Al]ZSM-5 (Si/Al = 25; PQ Corp.) by the incipient wetness impregnation technique from an aqueous solution of $FeCl_3$ [12] of a specified concentration (0.8 cm^3 of the solution per 1 g of zeolite dried at 60°C). Then the samples were dried at room temperature in air and calcined in vacuum conditions (0.1 torr) while ramping the temperature (100°C, 30 min; 200°C, 30 min; 250°C, 30 min; 300°C, 60 min; and 400°C, 30 min). No $FeCl_3$ sublimation (m.p. 296°C) was observed during this procedure. This means that the entire amount of impregnated iron was retained by the zeolite. After cooling the samples to room temperature, they were calcined at 520–530°C for 4 h in an air flow. We believe that the formation of isolated $FeCl_2^+$ species stabilized in the cationic positions of the zeolite occurs first in the course of such preparation. Upon oxidative calcination, these species are transformed into FeO^+ species [12].

H[Fe]ZSM-5 ferrisilicates. Two types of high-crystallinity ferrisilicates (MFI-1 and MFI-2) with the structure of ZSM-5 type were prepared by the synthesis of Na[Fe]ZSM-5 with further exchange of Na^+ ions for NH_4^+ and calcination at 650°C in an air flow. The total iron contents for both samples were approximately the

0023-1584/02/4301-0099$27.00

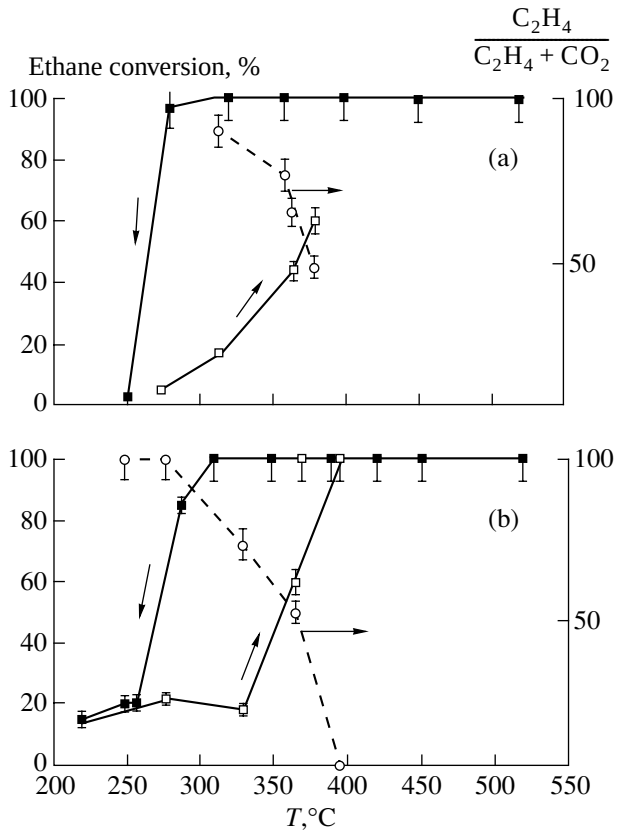

Fig. 1. Dependence of the catalytic activity and selectivity of (a) 0.5% Fe-H[Al]ZSM-5 and (b) 2.1% Fe-H[Al]ZSM-5 samples calcined at 520°C on the temperature of ethane oxidation by nitrous oxide.

same (SiO_2/ Fe_2O_3 = 22.5 and 19.5 for MFI-1 and MFI-2, these values corresponded to 3.9 and 4.6 wt % Fe) but the distribution of Fe^{3+} ions in these samples was radically different (the ratio of framework to extraframework Fe^{3+} ions was equal to ~8 and 0.6, respectively).

HZSM-5 zeolite. HZSM-5 zeolite with trace amount of iron (~0.005 wt % Fe) was used as a reference sample. The sample of NH_4ZSM-5 (Si/Al = 21, Na_2O < 0.1 wt %) prepared by ion exchange from NH_4ZSM-5 was dehydroxylated by the calcination in a dry air flow at 900°C. The prepared sample exhibited mainly Lewis acidity and possessed rather high crystallinity (>90% according to XRD).

Catalytic Tests

The loading of an air-dry sample (~90 mg, fraction 0.25–0.5 mm) was placed in a fixed-bed quartz microreactor (~ 0.2 cm^3) and calcined at 520°C in a dry air flow (50 cm^3/min) for 2 h. Then, the reaction mixture (21.5% N_2O + 2.3% C_2H_6 + 76.2% He or 6.3% N_2O + 93.7% He) was supplied in the reactor (GHSV = 1.5×10^4–2.0×10^4 h^{-1}, atmospheric pressure, T = 500–520°C). The reaction products were analyzed using a chromatograph equipped by TCD and a "Polysorb-1" column.

A series of measurements was performed with a stepwise temperature decrease from 500 to ~270°C. Then, the catalyst was cooled to 80–100°C and a series of measurements were carried out with a stepwise temperature increase up to 450–500°C. After the end of the experimental cycle, the sample was calcined in an air flow at 750°C for 2 h and then used in the next catalytic cycle.

TG–DT Analysis

Combined TG–DTG–DT analyses were performed on an MOM Derivatograph-C. The experiments were carried out under static air conditions with a linear temperature rise (10°C/min) up to 900°C. Both initial samples and the samples after the catalytic cycle were analyzed.

ESR Measurements

ESR spectra of Fe^{3+} ions and coke were measured at 20 and 250°C using a reflecting spectrometer (λ = 3.2 cm) and DPPH as a standard. The samples after the catalytic tests were placed into a glass ampule with an inner diameter of ~2 mm. Then, the ampule was placed in the resonator cavity and sealed to the vacuum-adsorption setup, which enables vacuum treatment at ~10^{-4} torr and N_2O adsorption.

RESULTS

C_2H_6 Oxidation with Nitrous Oxide

Fe-H[Al]ZSM-5. The reaction of C_2H_6 oxidation by N_2O on the Fe-H[Al]ZSM-5 samples with iron contents of 0.5 and 2.1 wt % activated at 520°C proceeds in two different directions depending on the reaction temperature (Fig. 1). The complete oxidation of ethane with a 100% conversion and 100% selectivity to CO_2 and H_2O is observed at 520°C. The total conversion and selectivity remain unchanged even after decreasing the temperature to 320°C. A further decrease in the temperature results in a dramatic drop of the catalyst activity and the selectivity to the products of complete oxidation. The appearance of C_2H_4 in light products leads to the enhancement of coke formation, and the catalyst becomes gray. When the temperature further increases, the ethane conversion turns out to be much lower than in the case of the descending temperature profile (Fig. 1). For instance, the total conversion of C_2H_6 at 360°C is below 50%. Moreover, the ethane conversion to CO_2 in this case is only 5–7% whereas the conversion to ethylene reaches 16–18%. The amount of CO_2 in the reaction products increases with the further growth in temperature, while the selectivity to the products of dehydrogenative oxidation diminishes (Fig. 1, dashed line).

The ratio of C_2H_4 to the sum $C_2H_4 + 2CO_2$ gives only an approximate value for the selectivity to C_2H_4 because the technique used for product analysis does not allow us to determine all the reaction products. However, the difference between the amount of converted ethane and the amount of ethane corresponding to the formation of the main products ($C_2H_4 + CO_2$), which is attributed to the products of coking and oxidative condensation, can be rather high in some cases (up to 40–50% of the total ethane conversion). A certain amount of high-molecular products are formed along with ethylene. These products deposit in the capillaries of the chromatographic system. In the case of prolonged measurements, these products can increase the dynamic resistance of the system and thus reduce the gas velocity.

Such dependences with a hysteresis presented in Fig. 1 are completely reproduced after the repetitive regeneration and coking of the sample. Thus, the state of the catalyst under conditions of coke formation is reproducible in the low-temperature reaction between C_2H_6 and nitrous oxide. Catalyst coking in the oxidative media ($N_2O/C_2H_6 = 9.3$ while the stoichiometric ratio is 7) is rather unexpected. The oxidative dehydrogenation of ethane becomes the major reaction path due to a significant decrease in the rate of complete oxidation at 300–350°C. The difference between the samples with iron contents of 0.5 and 2.1 wt % is observed only at low temperatures (220–280°C): the coked sample with the high iron content is more active in the oxidative dehydrogenation of ethane (Fig. 1).

The dehydroxylation of the catalyst (750°C, 2 h) does not influence significantly conversions in the $N_2O + C_2H_6$ mixture. The catalytic activity exhibits the hysteresis shape arising from catalyst coking (Fig. 2). The selectivity to ethylene formation on the coked samples remains unchanged (Fig. 2, dashed line). All the dependences are reproducible after the repetitive regeneration and coking of the catalyst.

H[Fe]ZSM-5. The catalysts H[Fe]ZSM-5 (MFI-1 and MFI-2 samples) activated at 520°C exhibit the same hysteresis behavior with two characteristic temperature regions in the oxidation of ethane by nitrous oxide (Fig. 3) as the FeH[Al]ZSM-5 system (Figs. 1 and 2). The complete oxidation of ethane into CO_2 and H_2O with 100% conversion is observed at $T \geq 420$°C. Lowering the temperature to 280–290°C does not result in any changes: the only reaction gaseous products are the products of complete oxidation. A further decrease in the temperature leads to coke formation and to a sharp decrease in the catalyst activity. Ethylene becomes the main reaction product. Upon a further temperature increase, the conversion of ethane is much lower than in the case of the descending branch of the activity vs. temperature dependence (Fig. 3). Oxidative dehydrogenation dominates under such conditions (250–300°C). The yield of CO_2 increases with the temperature growth, while the selectivity to the products of

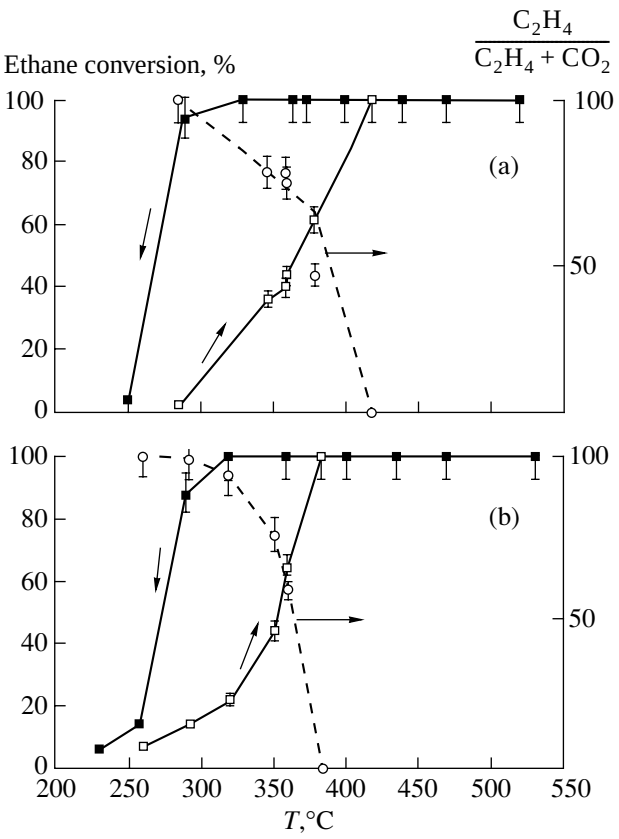

Fig. 2. Dependence of the catalytic activity and selectivity of (a) 0.5% Fe-H[Al]ZSM-5 and (b) 2.1% Fe-H[Al]ZSM-5 samples calcined at 750°C on the temperature of ethane oxidation by nitrous oxide.

oxidative dehydrogenation diminishes (Fig. 3, dashed line) similar to the case of the FeH[Al]ZSM-5 catalyst (Figs. 1, 2).

The dependences with hysteresis are reproduced after the subsequent regeneration and coking of the catalyst (Fig. 3). Nevertheless, the catalytic behavior of MFI-2 is quite different from that of the other samples: the formation of a significant amount of high-molecular products under conditions favorable for partial oxidation is observed. Rather fast deposition (within ~15 min) of these products in the chromatographic capillaries leads to the growth of the dynamic resistance of the system and complicates further measurements, because an increase in the gas pressure results in a corresponding increase in the volume of the gas sample taken for analysis. These carbon deposits cannot easily be extracted from the capillaries by a solvent such as *n*-hexane, but the use of the ethanol/acetone/CCl_4 (1 : 1 : 1) mixture enables us to wash the capillaries and to collect this fraction for further analysis.

Calcination of the MFI-1 and MFI-2 samples at 750°C for 2 h does not significantly influence the reaction of C_2H_6 oxidation by N_2O. The catalytic properties retain the hysteresis shape as a result of coke formation. The selectivity to ethylene on the coked samples

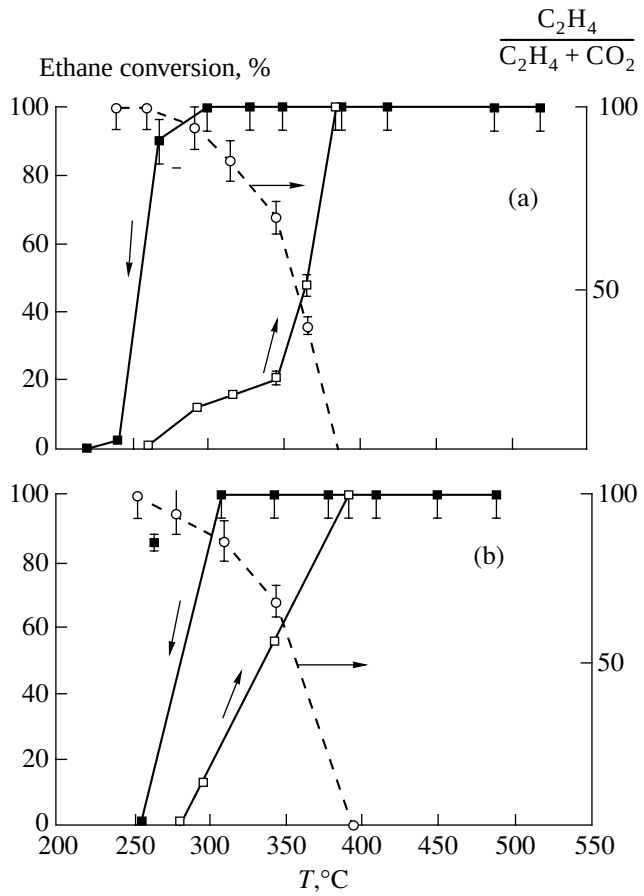

Fig. 3. Dependence of the catalytic activity and selectivity of (a) MFI-1 and (b) MFI-2 H[Fe]ZSM samples calcined at 520°C on the temperature of ethane oxidation by nitrous oxide.

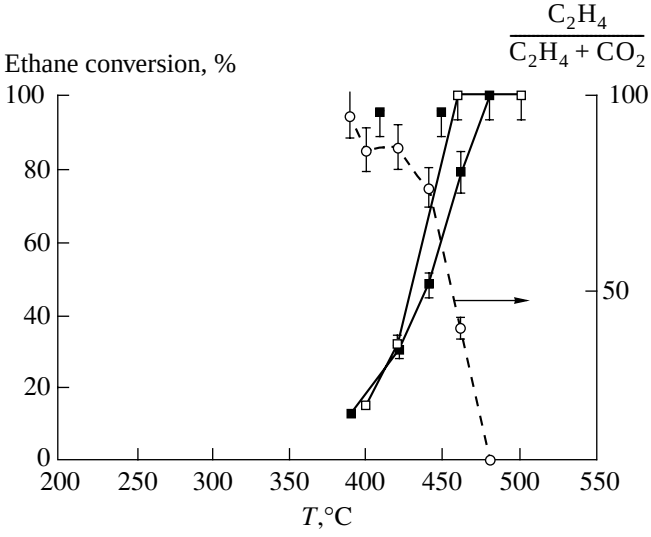

Fig. 4. Dependence of the catalytic activity and selectivity of the pure H[Al]ZSM-5 with trace amount of iron on the temperature of ethane oxidation by nitrous oxide.

remains unchanged (Fig. 3). At the same time, the rate of the formation of high-molecular products increases. These products deposited in the chromatographic capillaries complicate further catalytic measurements. The formation of oligomeric products could be monitored only qualitatively, but it should be noted that this process is faster on the ferrisilicate samples than on FeH[Al]ZSM-5. According to NMR, this heavy fraction contains only aliphatic oligomers and no aromatic compounds.

HZSM-5. The oxidation of C_2H_6 by nitrous oxide on the catalyst with only trace amounts of iron proceeds with a significant rate at much higher temperatures than on the other catalysts used (Fig. 4). The conversion of C_2H_6 on HZSM-5 at 380–390°C is below 10%, while even the coked FeH[Al]ZSM-5 and H[Fe]ZSM-5 catalysts are characterized by a higher ethane conversion at 300°C. Thus, the reaction rate on the pure HZSM-5 catalyst is considerably lower than on the iron-containing samples. The complete oxidation of C_2H_6 with 100% conversion is achieved on HZSM-5 at 500–460°C (Fig. 4). A decrease in the temperature to 420°C is followed by the rapid deactivation of the catalyst due to coke formation. Ethylene is the main reaction product under these conditions. The selectivity to C_2H_4 at 400°C is higher than 80% at an ethane conversion of ~15% (Fig. 4, dashed line). After cooling the reactor to 100°C in the reaction mixture, no hysteresis is observed with a further increase in the temperature. The temperature rise from 390 to 480°C is followed by the gradual growth in the yield of the products of complete oxidation, while the yield of ethylene drops to zero (Fig. 4).

N_2O Conversion

Treatment of the coked 0.5%Fe-HZSM-5 sample with the oxidative gas mixture (6.9% N_2O + He) at 360°C results in the formation of CO_2 in considerable amounts. No ethylene was found in the products. The initial conversion of N_2O on the coked catalyst is equal to 20–25% and then, after six consecutive measurements, it decreases to 15% (Fig. 5). Under the same conditions, the catalyst free from carbon deposits (after regeneration at 520°C in air) is almost inactive. Noticeable decomposition of N_2O on the pure catalyst is observed only at $T \geq 420$°C (Fig. 5). Thus, the presence of coke on the catalyst facilitates the decomposition of N_2O.

TG–DTA Data

Analyses were performed for the catalysts taken after the catalytic reaction at low temperatures when the partial oxidation of C_2H_6 proceeds.

Fe-H[Al]ZSM-5. According to the results of TG–DTA measurements, the weight loss in the temperature interval up to 250–300°C (water removal) makes up ~2 wt %. The burning of the coke in the case of 0.5% Fe-HZSM-5 results in the appearance of two exother-

mic effects with T_{max} 375 and 470°C and a weight loss of 4.6%. The 2.1% Fe-HZSM-5 sample is characterized by a lower temperature of the exothermic effect (T_{max} = 432°C) and the weight loss is 5.4 wt %. The repeated DTA–TG measurements for these samples after coke removal are characterized by the same water loss. This means that the samples retain the same water adsorption capacity after calcination.

H[Fe]ZSM-5. The burning of the coke in the case of MFI-1 occurs at T_{max} = 322°C with a weight loss of ~3 wt %. For the MFI-2 catalyst, the temperature of the exothermic effect is 310–320°C and the weight loss is ~3 wt %. The initial HZSM-5 sample shows no exothermic effects after calcination. After the catalytic tests, it is characterized by two exothermic effects (T_{max} = 375 and 578°C) and a weight loss of ~4 wt %.

ESR Spectra

The ESR spectra (20°C) of 0.5% Fe-HZSM-5 and 2.1% Fe-HZSM-5 calcined at 520°C are presented in Figs. 6a and 6b. Calcination at 750°C in air does not change the spectra of the 0.5% Fe-HZSM-5 sample (Fig. 6a). In the case of the 2.1% Fe-HZSM-5 catalyst, calcination leads to the formation of a rather broad signal with $g \cong 2.0$ (Fig. 6b, dashed line) in addition to the initial low-field spectral components.

After the catalytic reaction, these spectra underwent considerable changes: (a) the ESR signal with g = 4.3 became weak and low-field signals with $g \geq 5.6$ completely disappeared; (b) a new asymmetric signal with $g \cong 2.0$ and $\Delta H \cong 230$ E was formed; and (c) a broad symmetric singlet ($\Delta H \cong 9$ Oe, g = 2.0) corresponding to coke appeared. *In situ* calcination of the samples in an N_2O atmosphere (250°C, 1 h) does not change the ESR spectra. The regeneration of samples by calcination at 750°C in air results in the complete disappearance of the coke singlet while other ESR components remain unchanged. The ESR spectrum of the sample with 2.1 wt % Fe regenerated after the catalytic measurements is shown in Fig. 6c for comparison with the spectra of the initial samples.

The ESR spectra at 20°C of MFI-1 calcined at 520°C are presented in Fig. 7a. The calcination of the sample at 750°C in air results in a considerable decrease in the intensity of the signal with g = 4.3 and in the further broadening of the line with $g \cong 2.0$. The catalyst after the reaction is characterized by the ESR spectra with the asymmetric line ($g \cong 2.0$, $\Delta H \cong 230$ Oe) and symmetric singlet ($\Delta H \cong 9$ Oe, g = 2.0) typical of coke. The intensity of the ESR signal of coke does not change significantly after evacuation of the sample. The narrow signal of coke disappeared after the oxidative calcination of the sample at 750°C, while other ESR signals remain unchanged (Fig. 7b).

The ESR spectrum of the initial MFI-2 sample contains a broad signal with $g \cong 2.0$ and a weak signal with g = 4.3. The calcination of the sample at 750°C causes a decrease in the intensity of the signal with g = 4.3 and a broadening of the signal with $g \cong 2.0$. The ESR spectrum of the sample after the catalytic reaction with further regeneration is similar to the spectrum presented in Fig. 7b.

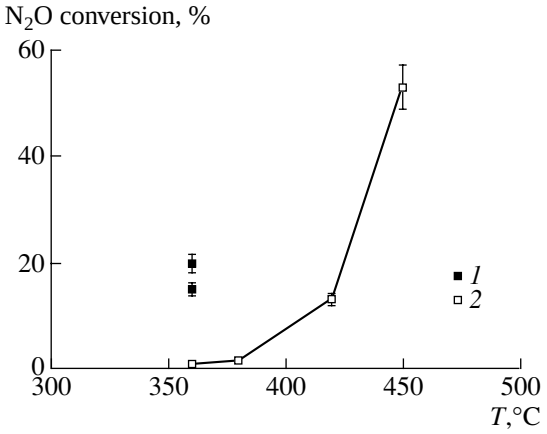

Fig. 5. Catalytic activity of 0.5% Fe-H[Al]ZSM-5 calcined at 750°C in decomposition of nitrous oxide: (*1*) coked sample, (*2*) the sample after regeneration.

DISCUSSION

Catalytic Oxidation of Ethane by Nitrous Oxide

It can be noted from the hysteresis dependences presented in Figs. 1–3 that the catalytic oxidation of ethane by excess N_2O on Fe-HZSM-5 at 250–350°C may proceed via two different pathways: the complete or partial oxidation of ethane. No significant difference was found between the catalytic properties of the iron-containing zeolite samples prepared by either direct synthesis or introducing iron ions in the cationic positions of H[Al]ZSM-5 (Figs. 1–3).

The activity of pure HZSM-5 containing ~0.03 wt % Fe is considerably lower in this reaction (Fig. 4) compared with iron-containing samples. The activity of the initial zeolite can be caused by either iron traces [13] or by the presence of defect redox [14] or Lewis sites [15]. However, the higher catalytic activity of Fe-HZSM-5 can be explained exclusively by the formation of iron species that are active in the oxidation of ethane. The question about the specific forms of stabilization of iron ions in the HZSM-5 zeolite matrix, for example, as a binuclear complex, has been actively discussed in the literature [8, 16–18]. Before the discussion of the results on the state of the catalyst, let us first discuss in more detail the character of the catalytic reaction occurring via two different routes.

High-Temperature Complete Oxidation of Ethane

Complete oxidation of C_2H_6 by nitrous oxide at $T > 380$°C on the Fe-HZSM-5 samples calcined at 520–750°C proceeds with a 100% conversion and does

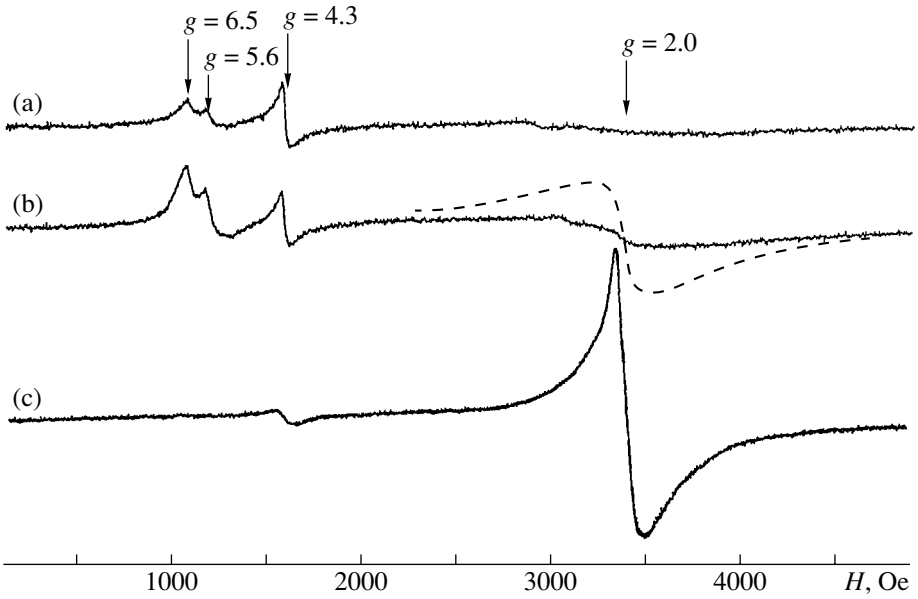

Fig. 6. ESR spectra of iron-containing samples at 20°C: (a) 0.5% Fe-H[Al]ZSM-5; (b) 2.1% Fe-H[Al]ZSM-5 (the dashed line corresponds to the spectrum after oxidative calcination at 750°C); (c) 2.1% Fe-H[Al]ZSM-5 regenerated after the catalytic cycle.

not depend on the temperature and time-on-stream (Figs. 1–3). No considerable suppression of the catalyst activity is observed at $T > 420$°C for a long time. CO_2 and H_2O are the only reaction products found at intermediate temperatures 350–280°C, and only coking of the catalyst causes the change of the reaction route.

We found earlier that the catalytic oxidation of ethane on Cu-HZSM-5 proceeds in two different ways depending on the oxidizing agents: oxygen [19] or nitrous oxide [11]. In the first case, it is a typical heterogeneous catalytic reaction [19], but when nitrous oxide is used [11], the catalytic behavior of the system was similar to that observed in this work: the existence of two different temperature regions was revealed. At temperatures above 420°C, the complete oxidation of ethane by nitrous oxide occurred with 100% selectivity and conversion and was independent of the temperature and time-on-stream. This situation is typical for mixed heterogeneous-homogeneous processes. The high-temperature reaction on Cu-HZSM-5 was accompanied by the glowing of the catalyst. This is an indication of the occurrence of chain oxidation processes with the participation of excited species [11].

Low-Temperature Reaction between C_2H_6 and N_2O on the Coked Catalysts

The low-temperature reaction (220–350°C) on all the coked Fe-HZSM-5 samples demonstrates some peculiarities. First, the significant extent of catalyst coking (3–5 wt % of coke) is observed even under oxidative conditions (excess N_2O). Second, the oxidative dehydrogenation and condensation (coking) become the dominant reactions on such catalysts characterized by a significantly different state of active surface compared with fresh samples. This leads to the suppression of complete oxidation in the case of the ascending branch of the hysteresis curve (Figs. 1–3). The coked Cu-HZSM-5 zeolites were found earlier to demonstrate a similar behavior [11].

The most noticeable difference in the catalytic activity of the samples is observed at low temperatures (230–300°C) when the selectivity to the products of oxidative dehydrogenation is rather high (Figs. 1–3). At 270–290°C, the sample containing 2.1 wt % Fe is 4–5 times more active than the sample with 0.5 wt % Fe (Fig. 1). The activity of the samples calcined at 750°C is lower but the ratio of the activities of these two samples remains the same (Fig. 2). Therefore, there is correlation between the activity and iron content for the catalysts of the same type. Comparison of these samples with ferrisilicates is rather difficult, because oligomer deposits are formed to a considerable extent in the case of MFI zeolites.

The Nature of Coke and Oligomer Deposits

DTA and ESR provide information on the nature of carbon deposits on the samples. The narrow ESR signal of coke for all samples is almost insensitive to the presence of oxygen, which is typical for amorphous and slightly graphitized carbon deposits. However, the amount of coke accumulated on the samples after catalytic tests of the same duration is considerably higher for samples containing Al in the zeolite matrix, and combustion of this type of coke proceeds at higher temperatures. These facts can be explained by the stronger Brønsted and/or Lewis acidity of H[Al]ZSM-5. Such

correlations are quite typical for the silicalites and HZSM-5 zeolites with different Al contents.

Thus, the amount of amorphous coke formed on MFI is smaller than that accumulated on Fe-H[Al]ZSM-5, and this coke can be oxidized at lower temperatures. At the same time, the formation of high-molecular products deposited in the capillaries of the chromatographic system for ferrisilicates is more intensive under the conditions of partial oxidation. According to NMR data, these deposits consist only of aliphatic oligomers and contain no aromatic moieties. The mechanism of their formation and migration is still unclear. The formation of peroxide entities and their further participation in the polymerization of ethylene hardly seems to be probable, even though peroxides cannot be detected by the analytical technique used in this work.

N_2O Conversion

Comparison of the activities of pure and coked 0.5% Fe-HZSM-5 samples (Fig. 5) clearly demonstrates that N_2O decomposition is enhanced in the presence of carbon deposits on the sample. However, the only product of "coke" oxidation by nitrous oxide at 360°C is CO_2, and no ethylene is formed from carbon deposits.

Iron Localization

ESR data provide valuable information on the state and distribution of iron in the samples. Fe-H[Al]ZSM-5 samples were investigated earlier [12, 20]; moreover, the quantitative approach to the investigation of Fe^{3+} ions by ESR was used in [12]. The spectra of the initial sample with g = 4.3, 5.6, and 6.5 (Fig. 6a) indicate that almost every iron ion in the sample containing 0.5 wt % Fe is stabilized in the cationic positions as isolated coordinatively unsaturated Fe^{3+} ions [12]. The concentration of isolated Fe^{3+} cations in the sample containing 2.1 wt % Fe is approximately the same, and the rest of Fe^{3+} atoms participate in the formation of Fe_2O_3 species (Fig. 6b). The oxidative calcination of samples at 750°C does not change the distribution of iron ions: the low-field ESR signals of isolated Fe^{3+} cations remain the same, whereas broadening of the signal with $g \cong 2.0$ (Fig. 6b, dashed line) indicates some growth of the Fe_2O_3 particles. It was shown earlier [12] that the reductive treatment of samples (1% H_2 + He; 400°C) leads to irreversible changes in the iron distribution and to the formation of the ferromagnetic Fe_3O_4 phase.

The catalytic oxidation of C_2H_6 with N_2O results in the formation of catalysts with a new distribution of iron ions. According to ESR data (Fig. 6c), isolated Fe^{3+} cations disappear completely under the conditions of the catalytic reaction and small paramagnetic clusters characterized by the narrow asymmetric singlet with $g \cong 2.0$ and $\Delta H \cong 230$ Oe are formed instead. No traces of ferromagnetic phases, which could be detected by such a sensitive method as ESR, were observed. *In situ* reoxidation of the samples in the atmosphere of N_2O (250°C, 1 h) and regeneration by calcination at 750°C in air does not promote the formation of isolated Fe^{3+} ions. Therefore, changes in the ESR spectra cannot be caused by the transformation of isolated ions into nonparamagnetic Fe^{2+} species. Thus, a new specific iron distribution, essentially different from the initial distribution, is formed during the catalytic reaction.

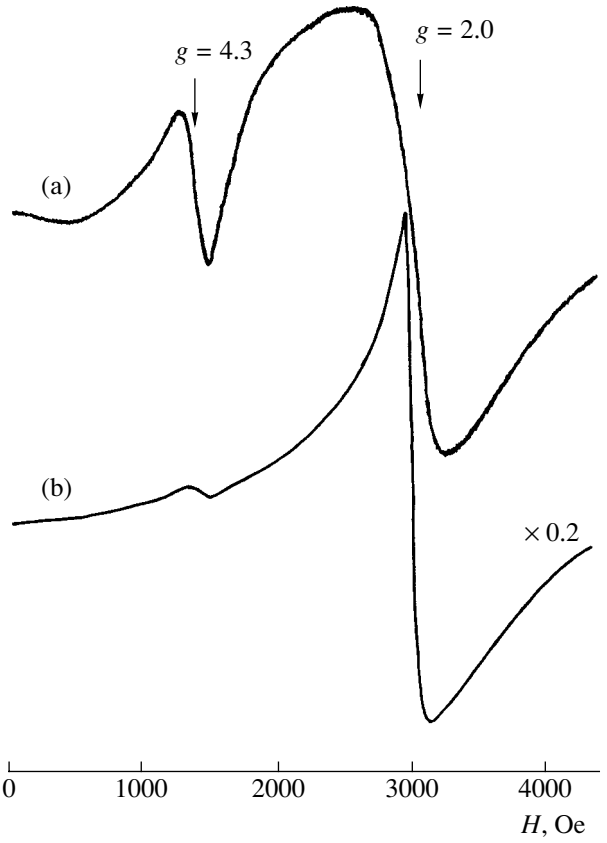

Fig. 7. ESR spectra of H[Fe]ZSM-5 (MFI-1) at 20°C: (a) initial sample, (b) the sample regenerated after the catalytic cycle.

Ferrisilicates have quite a different initial distribution of iron. ESR spectra of MFI-1 (Fig. 7a) indicate the simultaneous presence of iron species of both types: Fe_2O_3 crystallites and a considerable number of isolated Fe^{3+} ions stabilized in the framework of the zeolite (ESR signal with g = 4.3). The ratio between the framework and extraframework iron ions in the case of MFI-2 is much lower judging by the presence of the intense wide line with $g \cong 2.0$ and the weak signal with g = 4.3. However, the catalytic reaction (C_2H_6 + N_2O) causes a significant redistribution of iron in these samples. The share of framework iron ions becomes much lower. The samples after the catalytic cycle are characterized by the intense ESR signals with $g \cong 2.0$ and $\Delta H \cong 230$ Oe (Fig. 7b). This result indicates the forma-

tion of small paramagnetic clusters of the same type as in the case of Fe-H[Al]ZSM-5.

Thus, the catalytic reaction causes the formation of a new specific iron distribution, which is different from the initial distribution typical for air-calcined samples. The method of iron introduction and its initial distribution are unimportant.

ACKNOWLEDGMENTS

We would like to thank Dr. G. Vorbeck (Haldor Topsøe A/S, Lyngby, Denmark) for the samples and relevant information.

REFERENCES

1. Banares, M.A., *Catal. Today*, 1999, vol. 51, p. 319.
2. Ward, M.B., Lin, M.J., and Lunsford, J.H., *J. Catal.*, 1977, vol. 50, p. 306.
3. Aika, K.-I., Isobe, M., Kido, K., *et al.*, *J. Chem. Soc., Faraday Trans.*, 1987, vol. 83, p. 3139.
4. Hong, S.S. and Moffat, J.B., *Catal. Lett.*, 1996, vol. 40, p. 1.
5. Wang, Y. and Otsuka, K., *J. Catal.*, 1997, vol. 171, p. 106.
6. Erdohelyi, A. and Solymosi, F., *J. Catal.*, 1991, vol. 129, p. 497.
7. Suzuki, E., Nakashiro, K., and Ono, Y., *Chem. Lett.*, 1988, p. 953.
8. Kharitonov, A.S., Sobolev, V.I., and Panov, G.I., *Usp. Khim.*, 1992, vol. 61, p. 2062.
9. Kharitonov, A.S., Aleksandrova, T.N., Panov, G.I., *et al.*, *Kinet. Katal.*, 1994, vol. 35, no. 2, p. 296.
10. Sobolev, V.I., Dubkov, K.A., Paukshtis, Ye.A., and Panov, G.I., *Appl. Catal., A*, 1996, vol. 141, p. 185.
11. Kucherov, A.V., Kucherova, T.N., and Slinkin, A.A., *Kinet. Katal.*, 1992, vol. 33, no. 4, p. 877.
12. Kucherov, A.V. and Shelef, M., *J. Catal.*, 2000, vol. 195, p. 106.
13. Legliese, J., Petunchi, J.O., and Hall, W.K.J., *J. Catal.*, 1984, vol. 86, p. 392.
14. Slinkin, A.A., Larovskaya, T.K., Mishin, I.V., and Rubinshtein, A.M., *Kinet. Katal.*, 1978, vol. 19, no. 6, p. 922.
15. Mastikhin, V.M., Mudrakovskii, I.L., and Filimonova, S.V., *Chem. Phys. Lett.*, 1988, vol. 149, p. 175.
16. Ratnasamy, P. and Kumar, R., *Catal. Today*, 1991, vol. 9, p. 328.
17. Arbuznikov, A.V. and Zhidomirov, G.M., *Catal. Lett.*, 1996, vol. 40, p. 17.
18. Ovanesyan, N.S., Shteinman, A.A., Sobolev, V.I., *et al.*, *Kinet. Katal.*, 1998, vol. 39, no. 6, p. 863.
19. Kucherov, A.V., Kucherova, T.N., and Slinkin, A.A., *Kinet. Katal.*, 1992, vol. 33, no. 3, p. 618.
20. Kucherov, A.V., Montreuil, C.N., Kucherova, T.N., and Shelef, M., *Catal. Lett.*, 1998, vol. 56, p. 173.